ChemPubSoc Europe
DOI: 10.1002/open.201900295
Open Access ChemistryOPEN Communications

Bioinspired Healable Mechanochromic Function from Fluorescent Polyurethane Composite Film

Xiaoke Song[+],[a, b] Jun-Peng Wang[+],[a] Yan Song,[a] Tao Qi,*[a, b] and Guo Liang Li*[a, b]

Camouflage and wound healing are two vital functions for cephalopods to survive from dangerous ocean risks. Inspired by these dual functions, herein, we report a new type of healable mechanochromic (HMC) material. The bifunctional HMC material consists of two tightly bonded layers. One layer is composed of polyvinyl alcohol (PVA) and titanium dioxide (TiO_2) for shielding. Another layer contains supramolecular hydrogen bonding polymers and fluorochromes for healing. The as-synthesized HMC material exhibits a tunable and reversible mechanochromic function due to the strain-induced surface structure of composite film. The mechanochromic function can be further restored after damage because of the incorporated healable polyurethane. The healing efficiency of the damaged HMC materials can even reach 98% at 60 °C for 6 h. The bioinspired HMC material is expected to have potential applications in the information encryption and flexible displays.

In the long history of evolution, organisms have evolved a series of structures and functions to resist external invasion, remain healthy and prolong their lives. Bioinspired materials have been developed via variety synthetic strategies and nanostructures design.[1] Recently, mechanochromic materials for mimicking camouflage in nature were developed, which can exhibit changes in their optical properties in response to external forces.[2] For instance, mechanically active compounds can be incorporated into a polymer backbone to sense a force via the chemical reaction of the mechanophore[3] or a macromolecular packing change of the chains.[4] Mechanochromic composite materials containing functional nanoparticles were constructed based on Bragg diffraction or via tunable cracks and folds.[5] Healable materials mimicking self-healing function in nature can spontaneously repair damaged parts over multiple cycles based on supramolecular interactions.[6] For instance, layer-by-layer hydrogen bonding self-assembly has been used as an efficient strategy for the healing of hard and functional materials.[7]

Bioinspired materials with cooperating multiple functions in one system are highly desirable.[8] A superhydrophobic and mechanically durable biomimicking material was created by combining characteristics of the lotus leaf, mussel, and sandcastle worm.[9] Multifunctional materials with mechanical sensing and self-healing under magnetic fields[10] and multistimuli[11] were reported. The development of multifunctional materials that integrate mechanochromic and self-healing properties is highly demanded. Inspired by nature, camouflage and wound healing are two important skills for organisms to overcome danger.[12] For instance, the cephalopods have camouflage and wound healing bifunctions due to the muscle-controlled color changes and the reconstruction of proteins, respectively (Figure 1a).[5b,13] Herein, we report a new type of bioinspired healable mechanochromic (HMC) material that takes advantage of the multifunctional nature of biological systems. The HMC material is not only responsive to mechanical stimuli but also incorporates a self-healing function into one system (Figure 1b). The fabrication strategy was to construct hierarch-

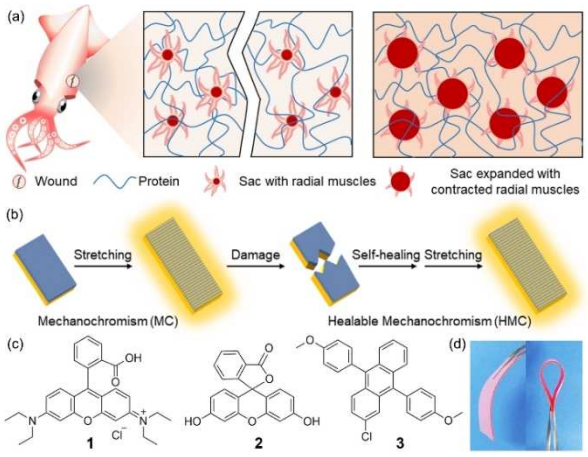

Figure 1. Structures and functions of the bioinspired healable mechanochromic (HMC) material. (a) The camouflage and wound healing bifunctions of cephalopods due to the muscle-controlled color changes and the reconstruction of proteins. (b) The HMC material with mechanochromic and self-healing bifunctions arising from hierarchical nanostructures. (c) The chemical structures of the fluorochromes of rhodamine B (**1**), fluorescein (**2**) and 9,10-bis(4-methoxyphenyl)-2-chloroanthracene (**3**), respectively. (d) The digital photos of the as-synthesized HMC material.

[a] X. Song,[+] Dr. J.-P. Wang,[+] Dr. Y. Song, Prof. T. Qi, Prof. G. Liang Li
National Engineering Laboratory for Hydrometallurgical Cleaner Production Technology
Institute of Process Engineering, Chinese Academy of Sciences
Beijing 100049, P. R. China
E-mail: glli@ipe.ac.cn
tqi@ipe.ac.cn
[b] X. Song,[+] Prof. T. Qi, Prof. G. Liang Li
University of Chinese Academy of Sciences
Beijing 100049, P. R. China
[+] These authors contributed equally to this work.

Supporting information for this article is available on the WWW under https://doi.org/10.1002/open.201900295

ical bilayer nanostructures with a PVA/TiO_2 layer and a fluorescent healable polymer layer. The opening/closing of the fluorescent 'gates' raising from the strain-induced cracks provides mechanochromism. Meanwhile, fluorescent healable polymers endow the HMC material with a dynamic self-healing function for advanced reversible encryption.

The fabrication approach of the HMC material is illustrated in Scheme S1. Initially, a PVA/TiO_2 layer (PVA/TiO_2 mass ratio = 1:4) with controlled thickness of 1.48 μm was prepared by spray coating. Separately, healable polymers were doped with fluorochromes for fabrication of a fluorescent healable layer (Figure S1, Supporting Information). Hierarchical bilayer composites were further constructed under vacuum conditions, followed by three stretching/releasing cycles to form dense uniform parallel gates.[14] A flexible composite film with distinguished bilayer structure is observed (Figure 1d). SEM images of the HMC material are shown in Figure S2a-c (Supporting Information).

The mechanochromic function of the HMC material is adjustable under the conditions of different strains. The mechanism is dependent on the strain-tunable surface gates in the PVA/TiO_2 layer.[5b] The fluorescence can be switched on and off under ultraviolet light due to the opening and closing of the gates when illuminated the PVA/TiO_2 layer, as shown in Figure 1b. Figure 2a shows optical micrographs of the HMC material at different strains and fluorescent photographs at the corresponding strains under 254 nm ultraviolet light. No eye-detectable fluorescence is observed without strain due to the closed gates. When the strain is increased from 0 to 100%, the emitted fluorescence becomes stronger with the change in the gates. The fluorescence spectra of the HMC material are shown in Figure 2b. The gate area ratio and characteristic peak at 597 nm corresponding to the fluorescent emission of the rhodamine B in the polymer layer are get stronger along with the strain enlargement (Figure S3, Supporting Information).[15]

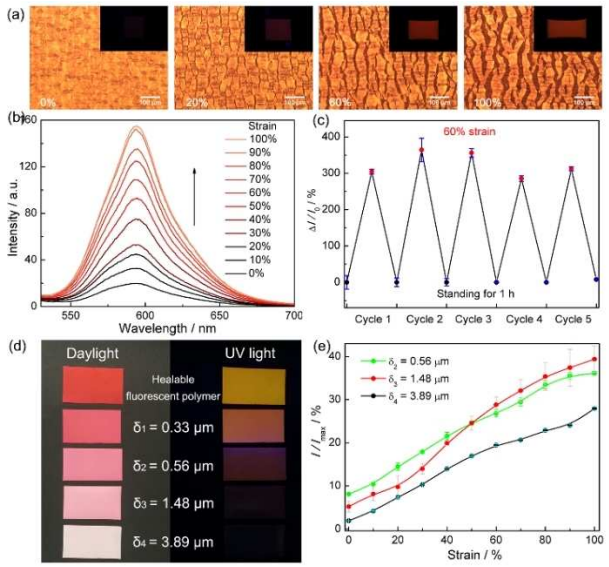

Figure 2. Mechanochromic property of the as-synthesized healable mechanochromic (HMC) material. (a) Optical micrographs of the HMC material at different strains; the insets are photographs at the corresponding strains under UV light. (b) Fluorescence spectra of the HMC material under different strains. (c) Repeatable mechanochromism of the HMC material after 60% strain application followed by standing for 1 h. (d) Digital images of the healable fluorescent polymer and HMC materials with different thicknesses of PVA/TiO_2 layers. (e) Relative fluorescence intensity of the HMC materials with different thicknesses of PVA/TiO_2 layers at strains from 0 to 100%.

Moreover, the HMC material exhibits excellent recovery performance. The fluorescence can change from the active state to the original dominant state once the strain is released (Figure S4, S5; Supporting Information). Within 30 seconds, the relative fluorescence intensity decreases to almost half of the original value under the condition of 100% strain. Five stretching/releasing cycles were carried out to reveal the reversible mechanochromic properties of the HMC material. As shown in Figure 2c, the relative fluorescence intensity of the HMC material remained changing with strain regularly and steadily.

To further regulate the mechanochromic function of the HMC material, composite films containing different PVA/TiO_2 layer thicknesses and TiO_2 contents were studied (Table S1, Supporting Information). As shown in Figure 2d, the healable fluorescent polymer before combining with the PVA/TiO_2 layer exhibits obvious fluorescence under UV light. The PVA/TiO_2 layer thicknesses were obtained by the side view SEM photos of the samples (Figure S6, Supporting Information). When the thickness of the PVA/TiO_2 layer increases from 0.33 μm to 3.89 μm, the color of the HMC material gradually changes from red to white. The static fluorescence correspondingly decreases with the thickness increase and is almost fully blocked for a thickness of 1.48 μm. But there is no effective shielding effect under UV light when the thickness is less than 0.56 μm. We collected the fluorescence intensity data of the characteristic peak at 597 nm and calculated the relative fluorescence intensity versus strain which plotted in Figure 2e. It shows that the relative fluorescence intensity increases with the strain for each sample. The sample with PVA/TiO_2 layer thickness of 1.48 μm changes the most from 0 to 100% strain. On the other hand, the increase of TiO_2 content contributes to the mechanochromic function due to the influence in the change of fluorescence before and after stretching. But an intact PVA/TiO_2 layer cannot be formed when the TiO_2 content up to 99 wt%. With increasing TiO_2 content, the number of nanoparticles changes from sparse to compacted corresponding to the fading of static fluorescence and formed a dense arrangement when the TiO_2 content reaches to 80 wt% with well shieling effect and maximum distinction on relative fluorescence intensity (Figure S7, S8, S9; Supporting Information). As discussed above, the HMC material of δ_3 with a PVA/TiO_2 layer thickness of 1.48 μm and TiO_2 content of 80 wt% shows contrasting change in fluorescence intensity. This sample was used in subsequent tests.

Based on the hierarchical hydrogen bonding interactions of 2-ureido-4[1H]-pyrimidinone, urethane, urea, samples ruptured by mechanical damage can recombined and recovered the structure integrity after healing (Figure 3a). The self-healing function of the HMC material was evaluated by mechanical tensile test. Two pieces of HMC material were contacted and treated. It could be observed from the side view SEM image

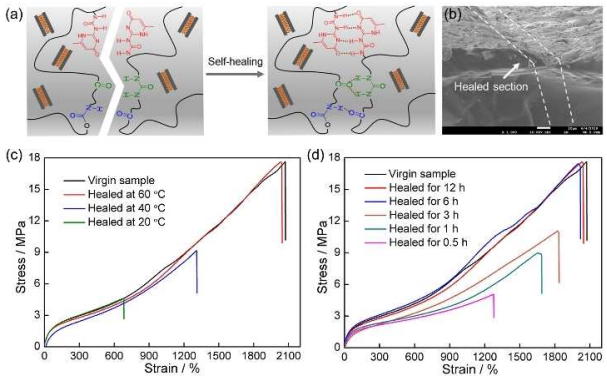

Figure 3. The self-healing function of the healable mechanochromic (HMC) material. (a) Scheme of the self-healing mechanism. (b) SEM image of the self-healing sample. Stress-strain curves of healable samples (c) after 24 h at different temperatures and (d) after different times at 60 °C.

that the damaged interfaces combined completely after self-healing (Figure 3b). The fractures at damaged interfaces are also recovered simultaneously without any exfoliation of PVA/TiO_2 layer (Figure S10, Supporting Information). The effects of the healing conditions on the self-healing function were further investigated as shown in Figure 3c and 3d. The self-healing efficiency increases with the healing temperature and healing time and was summarized in Table S2 (Supporting Information) and even reaches 98% when the specimen was healed at 60 °C for 6 h.

The switchable fluorescence ability is completely restored after self-healing. The damage and self-healing process are shown in Figure 4a. The healed specimen is integral and reveals obvious fluorescence under stretching (Figure 4b). The fluorescence spectra and relative fluorescence intensity at different strains were measured to quantitatively monitor the healable mechanochromic function which illustrated that the mechanochromism of the healed specimens is close to that of the virgin specimen (Figure 4c, S11, Supporting Information). Impressively, after three cycles of damage, healing, and stretching process carried out, the HMC material could recover without any performance loss (Figure 4d). These results imply that the mechanochromic function is fully restored after self-healing.

In addition, the construction of the HMC material is a general approach to obtain various healable mechanochromic materials through utilizing different fluorochromes such as rhodamine B, fluorescein and 9,10-bis(4-methoxyphenyl)-2-chloroanthracene into the healable polymer. These three types of HMC materials not only possess the self-healing function due to the healable matrix, but also exhibit orange, yellow and blue fluorescence under tension, respectively (Figure 5a).

Security encryption for information protection can be achieved by using composite materials under external stimuli.[5b,7c,16] High-level security encryption is required to protect information as the prevalence of informatization and digitization. The HMC material can obtain high level information storage by making information invisible and fragmented. As common encryption devices, information is invisible without certain stimuli for HMC material, and the intriguing feature is that we can break the information into parts and stored them separately. The decryption requires the bifunction of integration of fragmented encrypted information by self-healing and strain-induced fluorescent change due to mechanochromism (Figure 5c). Initially, a pattern of butterfly was broken into two pieces, each part of the pattern was embedded in a HMC film using fluorescent solution. The obtained encryption strips were connected and heated together at 60 °C for 24 h to assemble the whole encryption strip. After self-healing and stretching, the butterfly appeared due to the healable mechanochromic capability of the HMC material (Figure 5d). Furthermore, the HMC materials are expected to be useful in mechanical force sensing based on the relationship between the relative fluorescence intensity and stress by fitting the value corre-

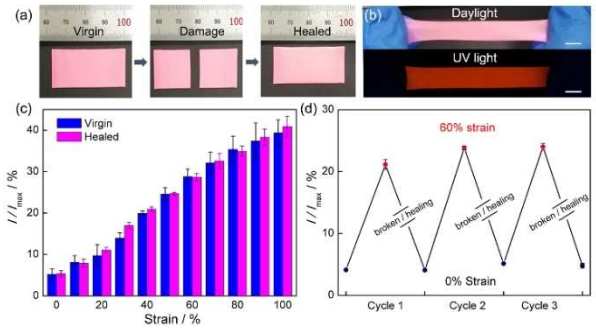

Figure 4. The mechanochromic function after self-healing of the healable mechanochromic (HMC) material. (a) The process of damage and self-healing. (b) The digital photo and fluorescent display of the healed specimen under tension. (c) Relative fluorescence intensity at different strains of the virgin and healed samples. (d) Reusability of the healable mechanochromic function of the bioinspired HMC material.

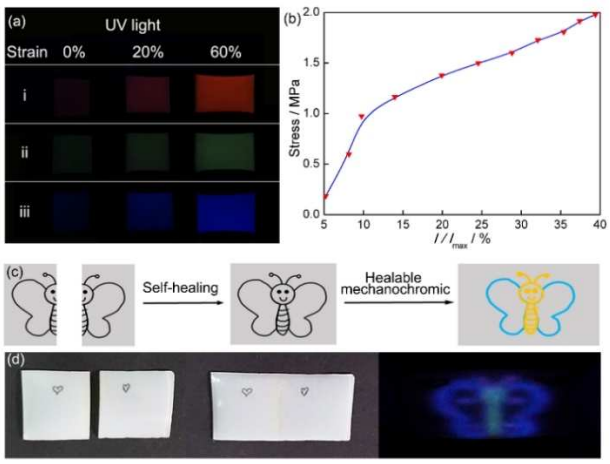

Figure 5. Applications of this type of the healable mechanochromic (HMC) material. (a) Extensive application of the HMC material for different fluorochrome-based HMC materials. The fluorochromes of i, ii and iii are rhodamine B, fluorescein and 9,10-bis(4-methoxyphenyl)-2-chloroanthracene, respectively. (b) Stress-relative fluorescence intensity curve of the HMC material. (c) Scheme of the high level encryption due to the healable mechanochromic function of the HMC material. (d) Separated, healed and stretched HMC materials for encryption.

sponding to certain strain respectively. (Figure 5b, S12, Table S3, Supporting Information).

In summary, the synthesis of a bioinspired HMC material including a PVA/TiO_2 layer and a healable fluorescent polyurethane has been demonstrated. The mechanochromic function can be tuned through the strain-induced opening and closing of the gates in the PVA/TiO_2 layer. Moreover, the mechanochromic function is almost restored after healing at 60 °C for 6 h due to the incorporated healable polymer layer. Due to the integration of mechanochromic and healing bifunctional properties, the HMC material is expected to have application in high level information encryption.

Experimental Section

Fabrication of HMC materials: the preparation of the fluorescent healable polymer composites is described below. Four grams of the synthesized healable polymer was dissolved in 60 mL of $CHCl_3$ (AR, Beijing Chemical Works) and stirred for 1.5 h at room temperature. Then, 0.5 mL of an ethanol solution of Rh–B (>99%, Aladdin, concentration of 0.01 g/mL) was added to the polymer solution and evenly stirred. The obtained fluorescent polymer solution was poured into a Teflon mold to evaporate the solvent overnight at room temperature. Finally, the fluorescent polymer film was dried under vacuum at 60 °C for 24 h. Fluorescent healable polymers with fluorochromes of fluorescein (95%, J&K Scientific Ltd.) and 9,10-bis (4-methoxyphenyl)-2-chloroanthracene (95%, Accela ChemBio Co., Ltd.) were also prepared according to the same approach.

The PVA/TiO_2 layer was prepared as follows. Around of 100 mg of PVA (M_w ~67000, Aladdin) was added to 10 mL of deionized water and stirred at 50 °C for 1 h. Then, 400 mg of TiO_2 nanoparticles (99%, Innochem) was added to the aqueous solution and stirred for 20 minutes. Then, an ultrasonic treatment was carried out for 20 minutes. After that, a spray pen with a 0.3 mm needle nozzle was utilized to spray the solution onto a dust-free polystyrene substrate surface. The work pressure of the spray pen was 0.48 MPa. The distance between the nozzle and substrate was approximately 20 cm. After drying at room temperature overnight, a composite layer was obtained. The TiO_2 content and shielding layer thickness were controlled by adjusting the TiO_2 concentration and total spraying amount, respectively.

The fluorescent healable polymer was cut into rectangular strips (40 mm × 20 mm) and placed on the PVA/TiO_2 layer. Then, the sample was heated in a vacuum oven at 50 °C for 36 h and peeled off from the substrate along the short side to obtain a well-bonded bilayer structure. Prestretching of 100% strain along the stripping direction was applied to the synthesized HMC material. After being fully released, the sample was ready for subsequent tests. The relative fluorescence intensity (I/I_{max}) was defined as the ratio of I to I_{max}, in which I is the intensity value at 597 nm in the fluorescence spectra of the HMC material at a given strain, I_{max} is the intensity value at 597 nm in the fluorescence spectra of the healable fluorescent polymer. For quantitative estimation of the healing efficiency (η), it was defined as

$$\eta = \sigma_{heal}/\sigma_{virgin} \times 100\,\%$$

where σ_{heal} and σ_{virgin} are the tensile strengths of the healed and virgin samples, respectively.

Characterization: the thickness of the composite films was measured as 350~400 μm by OU3600 thickness gauge (OUPU, China). The scanning electron microscope (SEM) images were obtained using a JSM-7610F thermal field-emission scanning electron microscope. Optical microscopy images were obtained using a Carl Zeiss Axio Scope A1. The fluorescence spectra were examined using a HITACHI F-4600 fluorescence spectrophotometer under excitation at 254 nm. The HMC materials were placed in a UV-III three-purpose ultraviolet (UV) analyzer viewing system under 254 nm for photographing or videotaping. Thermo gravimetric analysis (TGA) was carried out on the SEIKO TG-DTA6300 instrument. Samples (3~5 mg) were heated from 20 to 800 °C at the heating rate of 20 °C /min in nitrogen atmosphere. The mechanical properties were determined using an Instron 3365 universal testing machine with a stretching rate of 100 mm/min. Bone-like samples (active region: 4 mm × 3 mm × 0.4 mm) were prepared by cutting the HMC materials with a fixed shape cutter. ImageJ software was used to change the colour of the optical microscopy images into an 8-bit grayscale. The threshold was adjusted to the range of all the gate areas that could be selected. Then, the gate area ratio was automatically counted by the ImageJ software.

Acknowledgements

This work was funded by CAS Pioneer Hundred Talents Program and National Natural Science Foundation of China (Grant NO. 51803215 and 21975261).

Conflict of Interest

The authors declare no conflict of interest.

Keywords: mechanochromic · healable · bioinspired materials · bifunction

[1] a) M. Xuan, J. Shao, J. Zhao, Q. Li, L. Dai, J. Li, *Angew. Chem. Int. Ed.* **2018**, *57*, 6049–6053; *Angew. Chem.* **2018**, *130*, 6157–6161; b) Y. Li, X. Feng, A. Wang, Y. Yang, J. Fei, B. Sun, Y. Jia, J. Li, *Angew. Chem. Int. Ed. Engl.* **2019**, *58*, 796–800; c) F. Tao, Q. Han, P. Yang, *Langmuir* **2019**, *35*, 183–193.

[2] a) Z. Chi, X. Zhang, B. Xu, X. Zhou, C. Ma, Y. Zhang, S. Liu, J. Xu, *Chem. Soc. Rev.* **2012**, *41*, 3878–3896; b) E. A. A. Omar Rifaie-Graham, Livia K. Bast, Nico Bruns, *Adv. Mater.* **2018**, 1705483.

[3] a) D. A. Davis, A. Hamilton, J. Yang, L. D. Cremar, D. Van Gough, S. L. Potisek, M. T. Ong, P. V. Braun, T. J. Martinez, S. R. White, J. S. Moore, N. R. Sottos, *Nature* **2009**, *459*, 68–72; b) T. A. Kim, M. J. Robb, J. S. Moore, S. R. White, N. R. Sottos, *Macromolecules* **2018**, *51*, 9177–9183.

[4] a) W. E. Lee, C. L. Lee, T. Sakaguchi, M. Fujiki, G. Kwak, *Chem. Commun.* **2011**, *47*, 3526–3528; b) N. A. A. Rossi, E. J. Duplock, J. Meegan, D. R. T. Roberts, J. J. Murphy, M. Patel, S. J. Holder, *J. Mater. Chem.* **2009**, *19*.

[5] a) G. A. Williams, R. Ishige, O. R. Cromwell, J. Chung, A. Takahara, Z. Guan, *Adv. Mater.* **2015**, *27*, 3934–3941; b) S. Zeng, D. Zhang, W. Huang, Z. Wang, S. G. Freire, X. Yu, A. T. Smith, E. Y. Huang, H. Nguon, L. Sun, *Nat. Commun.* **2016**, *7*, 11802.

[6] a) X. Chen, M. A. Dam, K. Ono, A. Mal, H. Shen, S. R. Nutt, K. Sheran, F. Wudl, *Science* **2002**, *295*, 1698–1702; b) S. A. Hayes, F. R. Jones, K. Marshiya, W. Zhang, *Composites: Part A* **2007**, *38*, 1116–1120; c) A. M. Kushner, J. D. Vossler, G. A. Williams, Z. Guan, *J. Am. Chem. Soc.* **2009**, *131*, 8766–8768; d) P. Cordier, F. Tournilhac, C. Soulie-Ziakovic, L. Leibler, *Nature* **2008**, *451*, 977–980; e) S. Chen, W. H. Binder, *Acc. Chem. Res.* **2016**, *49*, 1409–1420; f) Y. Song, Y. Liu, T. Qi, G. L. Li, *Angew. Chem. Int. Ed.* **2018**, *57*, 13838–13842; g) S. Chen, N. Mahmood, M. Beiner, W. H. Binder, *Angew. Chem. Int. Ed.* **2015**, *54*, 10188–10192; *Angew. Chem.* **2015**, *127*, 10326–10330; h) A. Campanella, D. Dohler, W. H. Binder, *Macromol. Rapid Commun.* **2018**, *39*, 1700739.

[7] a) X. Wang, F. Liu, X. Zheng, J. Sun, *Angew. Chem. Int. Ed.* **2011**, *50*, 11378–11381; *Angew. Chem.* **2011**, *123*, 11580–11583; b) T. Yuan, X. Cui, X. Liu, X. Qu, J. Sun, *Macromolecules* **2019**, *52*, 3141–3149; c) M. Qin, M. Sun, R. Bai, Y. Mao, X. Qian, D. Sikka, Y. Zhao, H. J. Qi, Z. Suo, X. He, *Adv. Mater.* **2018**, *30*, 1800468.

[8] a) A. C. Balazs, T. Emrick, T. P. Russell, *Science* **2006**, *314*, 1107–1110; b) W. Huang, D. Restrepo, J. Y. Jung, F. Y. Su, Z. Liu, R. O. Ritchie, J. McKittrick, P. Zavattieri, D. Kisailus, *Adv. Mater.* **2019**, 1901561; c) N. A. Yaraghi, D. Kisailus, *Annu. Rev. Phys. Chem.* **2018**, *69*, 23–57; d) D. Shchukin, H. Möhwald, *Science* **2013**, *341*, 1458–1459; e) A. R. Studart, *Angew. Chem. Int. Ed.* **2015**, *54*, 3400–3416; *Angew. Chem.* **2015**, *127*, 3463–3479.

[9] K. Han, T. Y. Park, K. Yong, H. J. Cha, *ACS Appl. Mater. Interfaces* **2019**, *11*, 9777–9785.

[10] A. S. Ahmed, R. V. Ramanujan, *Sci. Rep.* **2015**, *5*, 13773.

[11] G. Weng, S. Thanneeru, J. He, *Adv. Mater.* **2018**, *30*, 1706526.

[12] a) C. E. Diesendruck, N. R. Sottos, J. S. Moore, S. R. White, *Angew. Chem. Int. Ed.* **2015**, *54*, 10428–10447; *Angew. Chem.* **2015**, *127*, 10572–10593; b) P. Fratzl, *J. R. Soc. Interface* **2007**, *4*, 637–642; c) M. Stevens, S. Merilaita, *Phil. Trans. R. Soc. B* **2009**, *364*, 423–427.

[13] a) R. A. Cloney, E. Florey, *Z. Zellforsch. Mikrosk. Anat.* **1968**, *89*, 250–280; b) A. Pena-Francesch, M. C. Demirel, *Front. Chem.* **2019**, *7*, 69; c) D. Gaddes, H. Jung, A. Pena-Francesch, G. Dion, S. Tadigadapa, W. J. Dressick, M. C. Demirel, *ACS Appl. Mater. Interfaces* **2016**, *8*, 20371–20378; d) P. Imperadore, G. Fiorito, *Front. Physiol.* **2018**, *9*, 593; e) J. L. Polglase, A. Bullock, R. Roberts, *J. Zool.* **1983**, *201*, 185–204; f) R. A. Clark, K. Ghosh, M. G. Tonnesen, *J. Invest. Dermatol.* **2007**, *127*, 1018–1029; g) Y. Di, R. J. Heath, *Polym. Degrad. Stab.* **2009**, *94*, 1684–1692.

[14] a) C. H. Hsueh, M. Yanaka, *J. Mater. Sci.* **2003**, *38*, 1809–1817; b) W. G. Mao, Y. Y. Chen, Y. J. Wang, M. Zhou, H. Y. Yang, Z. Wang, C. Y. Dai, X. Chen, D. N. Fang, *Surf. Coat. Technol.* **2018**, *350*, 211–226.

[15] M. Handke, T. Adachi, C. Hu, M. D. Ward, *Angew. Chem. Int. Ed.* **2017**, *56*, 14003–14006; *Angew. Chem.* **2017**, *129*, 14191–14194.

[16] a) H. H. Pham, I. Gourevich, J. K. Oh, J. E. N. Jonkman, E. Kumacheva, *Adv. Mater.* **2004**, *16*, 516–520; b) K. Zhong, J. Li, L. Liu, S. Van Cleuvenbergen, K. Song, K. Clays, *Adv. Mater.* **2018**, *30*, 1707246.

Manuscript received: September 27, 2019
Revised manuscript received: November 20, 2019